7-2018

Asymmetric Hillslope Erosion Following Wildfire in Fourmile Canyon, Colorado

Edward R. Abrahams

James M. Kaste
William & Mary, jmkaste@wm.edu

William Ouimet

David P. Dethier

Recommended Citation

Abrahams, Edward R.; Kaste, James M.; Ouimet, William; and Dethier, David P., Asymmetric Hillslope Erosion Following Wildfire in Fourmile Canyon, Colorado (2018). *Earth Surface Processes and Landforms*, 43(9), 2009-2021.
https://doi.org/10.1002/esp.4348

SPi | Journal Code: E S P | Article ID: 4 3 4 8 | Dispatch: 22.02.18 | CE: | No. of Pages: 13 | ME:

EARTH SURFACE PROCESSES AND LANDFORMS
Earth Surf. Process. Landforms (2018)

Published online in Wiley Online Library
(wileyonlinelibrary.com) DOI: 10.1002/esp.4348

Asymmetric hillslope erosion following wildfire in Fourmile Canyon, Colorado

Q2 Q1 Edward R. Abrahams,[1] James M. Kaste,[1]* William Ouimet[2] and David P. Dethier[3]
[1] Department of Geology, The College of William & Mary, Williamsburg, VA USA
[2] Geography and Center for Integrative Geosciences, University of Connecticut, Storrs, CT USA
[3] Department of Geosciences, Williams College, Williamstown, MA USA

Received 30 November 2016; Revised 27 November 2017; Accepted 15 January 2018

*Correspondence to: James M. Kaste, Department of Geology, The College of William & Mary, 217 McGlothlin Hall, Williamsburg, VA 23187, USA. E-mail: jmkaste@wm.edu

ESPL
Earth Surface Processes and Landforms

ABSTRACT: Infrequent, high-magnitude events cause a disproportionate amount of sediment transport on steep hillslopes, but few quantitative data are available that capture these processes. Here we study the influence of wildfire and hillslope aspect on soil erosion in Fourmile Canyon, Colorado. This region experienced the Fourmile Fire of 2010, strong summer convective storms in 2011 and 2012, and extreme flooding in September 2013. We sampled soils shortly after these events and use fallout radionuclides to trace erosion on polar- and equatorial-facing burned slopes and on a polar-facing unburned slope. Because these radionuclides are concentrated in the upper decimeter of soil, soil inventories are sensitive to erosion by surface runoff. The polar-facing burned slope had significantly lower cesium-137 (^{137}Cs) and lead-210 (^{210}Pb) inventories ($p < 0.05$) than either the polar-facing unburned slope or equatorial-facing burned slope. Local slope magnitude does not appear to control the erosional response to wildfire, as relatively gently sloping (~20%) polar-facing positions were severely eroded in the most intensively burned area. Field evidence and soil profile analyses indicate up to 4 cm of local soil erosion on the polar-facing burned slope, but radionuclide mass balance indicates that much of this was trapped nearby. Using a ^{137}Cs-based erosion model, we find that the burned polar-facing slope had a net mean sediment loss of 2 mm (~1 kg m^{-2}) over a one to three year period, which is one to two orders of magnitude higher than longer-term erosion rates reported for this region. In this part of the Colorado Front Range, strong hillslope asymmetry controls soil moisture and vegetation; polar-facing slopes support significantly denser pine and fir stands, which fuels more intense wildfires. We conclude that polar-facing slopes experience the most severe surface erosion following wildfires in this region, indicating that landscape-scale aridity can control the geomorphic response of hillslopes to wildfires. Copyright © 2018 John Wiley & Sons, Ltd.

KEYWORDS: soil; erosion; fallout; radionuclides; wildfire

Introduction

To fully understand how the critical zone evolves over time, we need to quantify how weathering and erosion rates are impacted by environmental factors (Brantley *et al.*, 2016). Wildfires are one factor that is predicted to increase in frequency with changing climate conditions in the coming years (Westerling *et al.*, 2006). Fires play a crucial role in critical zone processes, as they can instantly impact vegetation cover, soil properties, and drainage characteristics, often making landscapes much more prone to erosion (Campbell *et al.*, 1977; Nyman *et al.*, 2013). Sufficiently intense wildfires induce hyper-dryness in soils, leading to soil hydrophobicity and soil repellency, which have been shown to reduce infiltration by orders of magnitude for a period of up to five years after the burn (Doerr *et al.*, 2000; Moody and Martin, 2001; Shakesby and Doerr, 2006). As a result of these effects, hillslopes become much more susceptible to rainsplash and overland flow after wildfires, leading to runoff that degrades stream water quality (Murphy *et al.*, 2015).

While it is well established that soil erosion may follow wildfires, the geomorphic response to fire often depends on several landscape factors. Slope gradient, hillslope position, and specifically hillslope aspect play an important role in controlling the geomorphic response of hillslope soils to fire. Hillslope position, for example, was the best predictor of the frequency and magnitude of sediment transport in a sub-alpine eucalypt forest in south-eastern Australia, with lower positions on a burned slope experiencing greater erosion and slower regrowth than higher ones. Erosion on an adjacent unburned slope, in contrast, had no relationship with landscape position (Smith and Dragovich, 2008). In a comparison of burned and unburned slopes in central Idaho, Perreault *et al.* (2017) investigated the Q4 Q5 effects of several hillslope terrain factors, including slope position, gradient, curvature, and aspect, on soil loss after a fire. They observed a weak relationship between slope position and soil loss, while neither gradient nor curvature showed significant relationships. Erosion magnitude was notably correlated with hillslope aspect on unburned slopes, due to the hillslope asymmetry present in the study area, though this difference was absent on burned slopes.

Hillslope asymmetry is a widespread phenomenon in mountainous landscapes wherein opposing hillslopes have significantly different characteristics. Marqués and Mora (1992) measured sediment transport during multiple high intensity precipitation events on a pair of burned asymmetrical hillslopes in the Montserrat region of Spain, finding stark differences in erosional regimes between the two. Though both sites were of similar slope and substrate, the drier, less vegetated south-facing (equatorial-facing) slope had erosion rates that were six times higher than those on the north-facing (polar-facing) slope, which exhibited an increased resistance to erosion after the first rainfall event due to quick regrowth and a lack of rilling. Hillslope asymmetry is also typical throughout the American Cordilleran, where opposing hillslopes differ not only in vegetative cover, but in slope angle as well (Poulos *et al.*, 2012). The processes that regulate slope angle differences are widely attributed to microclimate-induced changes to vegetation cover and soil moisture properties (e.g. Burnett *et al.*, 2008), but direct measurements of sediment transport rates on opposing hillslopes in these asymmetrical valleys are needed to quantify the actual effects of fire, particularly for extreme geomorphic events.

Here we investigate hillslope erosion in Fourmile Canyon, Colorado following the September 2010 wildfire and strong precipitation events in 2011–2014. In this part of the Colorado Front Range, lower moisture on the equatorial-facing slopes limits plant growth, while polar-facing slopes are densely forested (Peet, 1981). We measure soil inventories of fallout radionuclides beryllium-7 (^{7}Be), cesium-137 (^{137}Cs) and lead-210 (^{210}Pb) on opposing hillslopes with the goal of measuring how landform-scale aridity differences control the magnitude of the geomorphic response to wildfire (Sheridan *et al.*, 2016). Given that polar-facing slopes in this region are steeper and have considerably more vegetation than equatorial-facing hillslopes (Anderson *et al.*, 2011; Befus *et al.*, 2011; Hinckley *et al.*, 2012), we hypothesize that this asymmetry drives more severe burn intensity and subsequent erosion on the polar-facing slopes.

Regional Setting

Fourmile Canyon

Fourmile Canyon, in north-central Colorado's Front Range, contains Fourmile Creek, a tributary to Middle Boulder Creek (Figure 1) and has many features typical of Front Range landscapes. The Fourmile catchment is characterized by steep terrain (average slope > 35%), which locally exceed 100%, particularly on polar-facing slopes (Graham *et al.*, 2012). The geology of the upper basin is primarily Proterozoic metamorphic gneiss and schist, while the lower basin is predominantly underlain by the Boulder Creek Granodiorite; soils derived from this bedrock generally have a gravelly sand texture (Moody and Martin, 2015). Proterozoic and Phanerozoic intrusions containing metallic ores are present throughout the area (Lovering and Goddard, 1950). Ore deposits have been the focus of past gold mining operations in the basin, resulting in mining legacy deposits along the creek, and on the slopes of Fourmile Canyon (Murphy, 2006).

Fourmile Canyon lies almost entirely within the lower montane vegetation zone (1830–2440 m), in which stands of Ponderosa pine and Douglas fir, along with numerous understory species, are the most common plant cover (Kaufmann *et al.*, 2006; Graham *et al.*, 2012). Some understory species are readily flammable when dried, such as cheatgrass, an invasive grass that is now common in the area (Graham *et al.*, 2012). In Fourmile Canyon, polar-facing slopes tend to get less direct sun than equatorial-facing ones, and are thus relatively more moist (Hinckley *et al.*, 2012). Because of this, aspect has a strong control on aridity and thus vegetative cover (Anderson *et al.*, 2011). Plant cover on polar-facing slopes is much denser than on the opposing slope; polar aspects are covered by dense Ponderosa pine, Limber pine and Douglas fir forests, while equatorial aspects exhibit more open sparse stands of Ponderosa pine, with a thicker understory consisting of Rocky Mountain juniper and grasses (Veblen *et al.*, 2000; Graham *et al.*, 2012; Ebel *et al.*, 2015). Fourmile Canyon's equatorial-facing (northern) slope and polar-facing (southern) slopes differ significantly in their profiles; equatorial-facing slopes have a lower gradient while polar-facing slopes are markedly steeper (Figure 2) (Foster *et al.*, 2015).

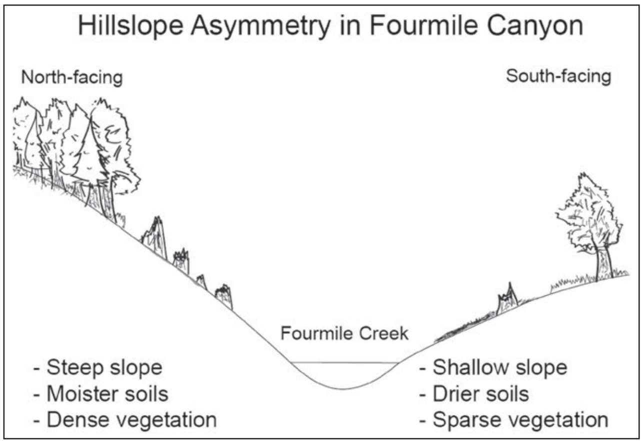

Figure 2. Hillslope asymmetry in Fourmile Canyon; steeper north-facing slopes have denser stands of pine.

Colour online, B&W in print

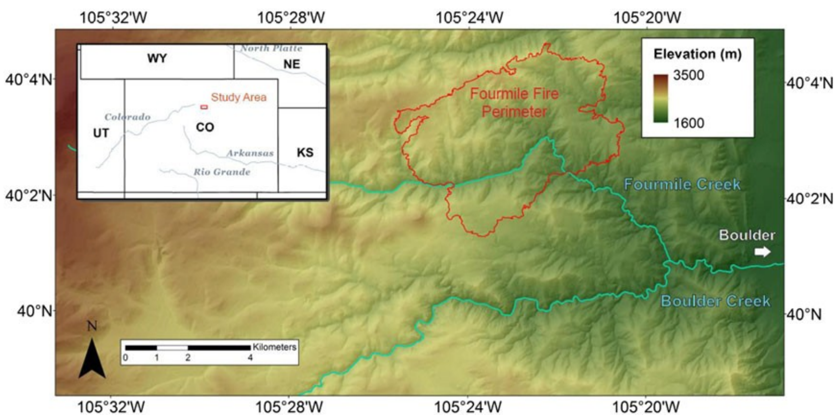

Figure 1. Elevation map of Fourmile Canyon region with fire perimeter outlined in red. [Colour figure can be viewed at wileyonlinelibrary.com]

Fourmile Canyon experiences both wildfires, which are common along the Colorado Front Range (Veblen *et al*., 2000), and strong convective summer storms with monsoon moisture coming from the Gulf of California (Douglas *et al*., 2004). In September of 2010, the Fourmile Canyon Fire burned ~25 km^2 of land (Figure 1) in and around the slopes of Fourmile Canyon (Figure 3). Beginning on September 6, 2010 and continuing intermittently for the next four days, it destroyed 168 homes, more than any previous fire in Colorado's history. With a perimeter that came as close as six miles to Boulder, the Fourmile Canyon Fire was one of the most expensive fires in the region's history (Graham *et al*., 2012). In 2011 and 2012, strong summer convective storms with high intensity (maximum 30-minute rainfall intensity > 10mm/h) hit the area, and Fourmile Creek discharge was measured to be several times higher than discharge produced by comparable storms prior to the fire (Murphy *et al*., 2015). Following these events, in September 2013, the Colorado Front Range experienced abnormally heavy rains, which led to massive flooding in Fourmile Canyon and other areas along Boulder Creek, during the 2013 Colorado Floods. Within a seven-day period, the burned portion of Fourmile Canyon received 210–370 mm of precipitation (Murphy *et al*., 2015), which is approximately half of the mean annual rainfall there (550 mm) and instigated over a thousand debris flows (Rengers *et al*., 2016). The regional flooding that resulted from these rains had a frequency on the order of 50 to 100 years (Yochum, 2015).

Materials and Methods

Short-lived radionuclides on catena transects

Sediment tracers can provide unique insights into transport processes operating on timescales of < 1 yr to decades (Walling and He, 2001; Smith *et al*., 2013; Perreault *et al*., 2017), and we apply these here to study the control that hillslope aspect has on post-fire erosion response. Short-lived radionuclides that are delivered to landscapes primarily via rainfall (e.g. 'fallout radionuclides') and adhere to soil particles are commonly used to quantify and trace soil erosion processes (Wallbrink and Murray, 1996; Walling and He, 1999; Mabit *et al*., 2008). Naturally-occurring cosmogenic ^{7}Be ($T_{1/2}$ = 53 days) and atmospheric ^{210}Pb ($^{210}Pb_{ex}$, hereafter; $T_{1/2}$ = 22 years) are introduced to vegetation and upper-most 1–2 cm of topsoil with rainfall at a relatively constant rate each year (Landis *et al*., 2014), and the weapons-testing era fission product ^{137}Cs ($T_{1/2}$ = 30 years) was introduced in a pulse during 1956–1967 (Ritchie and McHenry, 1990). In moderately dry climates (annual precipitation < 1 m), limited leaching rates of cosmogenic ^{7}Be, weapons-derived ^{137}Cs and $^{210}Pb_{ex}$ concentrate the nuclides in the upper decimeter of soil, making them powerful tracers of topsoil erosion (Pelletier *et al*., 2005; Kaste *et al*., 2016). Points on the landscape with low radionuclide inventories compared to levels supported by atmospheric deposition record soil loss, while points with relatively high radionuclide inventories are caused by local soil accumulation.

A range of detailed models that relate nuclide inventories to erosion rates are available (e.g. Walling and He, 1999), but this method should be applied with caution particularly in areas impacted by wildfire (Parsons and Foster, 2011; Smith *et al*., 2013). The deposition of fallout is not uniform; spatial heterogeneity of fallout deposition on arid and semi-arid landscapes is controlled by small-scale (~1–10 m) rainshadowing effects and measured via coefficient of variation (CV) to be 10–35% (Kaste *et al*., 2006; Kaste *et al*., 2011). The spatial variation of atmospheric deposition must be measured using a reference site and applied as an uncertainty to the reference inventory (Kaste *et al*., 2016). Another pitfall associated with the radionuclide tracer technique is possible chemical mobility, particularly with ^{137}Cs in organic rich soils (Livens *et al*., 1996). Because ^{137}Cs is a monovalent cation with a hydration shell, it can be readily exchanged in soils and desorbed easily into soil solution by K^+, NH^{4+}, or H^+, and in some environments even be taken up by plants (Papastefanou *et al*., 2005). However, ^{210}Pb is much more particle reactive and has far less chance of geochemical mobility (Landis *et al*., 2014) and thus can be used in conjunction with ^{137}Cs as a means to check for possible chemical losses.

Smith *et al*. (2013) assess the strengths and weaknesses of several methods to trace sediment movement after fires, including fallout radionuclides. In coniferous forest environments, the surface concentrations for common tracers like ^{137}Cs and $^{210}Pb_{ex}$ have a tendency to increase after fire, as the radionuclide fraction previously contained in soil organic matter, largely surface material, is converted to ash. The combustion can also reduce soil mass, which enhances the effect of the additional radionuclides on their soil concentration (Reneau *et al*., 2007). These trends combined can change their concentration by an order of magnitude, and also tend to increase the spatial variability of the radionuclides, though this effect is more pronounced in $^{210}Pb_{ex}$ than ^{137}Cs. Overall, Smith *et al*. (2013) note that the primary considerations one should make when using radionuclide sediment tracers to compare burned and unburned areas are the magnitude of radionuclide concentration

Colour online, B&W in print

Figure 3. A significant difference in pine and fir density is apparent in these photographs of the polar (north)-facing burned slope (NFB) (left) and equatorial (south)-facing burned slope (SFB) (right) hillslopes taken in 2014. NFB is shown looking down-canyon and SFB is shown looking up-canyon. Both slopes burned during the Fourmile Fire in 2010, though more intensely on NFB, and both have begun the process of succession. [Colour figure can be viewed at wileyonlinelibrary.com]

increase associated with the burn, the persistence of this change over time, and particularly, the relative fraction of radionuclides stored in ash to those within the soil. If the amount of radionuclide in the combustible litter layer is high, then the movement of ash could lead to an overestimate of soil movement. We measure the radionuclide inventory in the combustible (O) layer and mineral soil in unburned reference areas adjacent to the burned slope to evaluate how these processes might affect our geomorphic interpretations.

We collected soil samples along hillslope catena transects in Fourmile Canyon in July, 2014 for short-lived radionuclides, which we use to trace and quantify recent transport and soil erosion. Our catena transects were designed to test the hypothesis that aspect controlled the hillslope erosion response from the storms that followed the 2010 wildfire. These transects were roughly centered around Wood Mine, a site that hosted a temporary US Geological Survey (USGS) gaging station that was destroyed during both the 2011 and 2013 floods, approximately 2.5 km above the town of Salina Junction (Figure 4). Because of its short half-life, soil inventories of ^{7}Be are controlled by processes that occurred in the ~6 months prior to our collection. However, soil inventories of ^{210}Pb and ^{137}Cs that we measured in 2014 reflect transport processes operating over the last few decades. Given the intense 2010 wildfire and subsequent storms in the years following this event, and the extraordinary sediment loads measured in Fourmile Creek during these years (Murphy *et al.*, 2015), we expect that much of the hillslope erosion and sediment movement that we traced in 2014 occurred during 2011–2013.

Hillslope catena transects were collected along downslope hillslope paths that started at local ridgetops. One transect was along a polar (north)-facing unburned slope (NFUB), and the other two were along a polar-facing burned slope (NFB) and an equatorial (south)-facing burned slope (SFB) (see photographs in Figure 3). All sampling points on NFB were in locations that were judged to have substantially burned, with complete vegetation loss based on field evidence (Figure 3), and this was corroborated by satellite photographs showing no vegetation along the entire NFB transect (Figure 4). We did not consider that the ridgetop on NFB was large enough to fully represent low slope areas, so we collected additional samples on a similar, nearby polar-facing slope that also burned in 2010 (NFB Upper). Sampling positions on NFUB were in dense vegetation (Figure 4).

An independent means of quantifying the burn history of the study area is based on burn intensity maps that were generated for Fourmile Canyon by the Monitoring Trends in Burn Severity (MTBS) project. MTBS utilizes the Fire Effects Monitoring and Inventory System (FIREMON), developed by Lutes *et al.* (2006) with the intention of creating a standardized procedure for analysis of wildfires. This is achieved using a metric called the differenced Normalized Burn Ratio (dNBR), which is produced by computing the difference between pre- and post-burn spectral data (Lutes *et al.*, 2006), and classified into a severity index using Landsat bands 4 and 7 (Miller and Thode, 2007; Eidenshink *et al.*, 2007). For our analysis, we assigned numbers to the four levels of burn severity present in our study area to calculate statistics for each slope, as shown in Figure 4 and Table I. The dNBR data for our transects indicated that the

Colour online, B&W in print

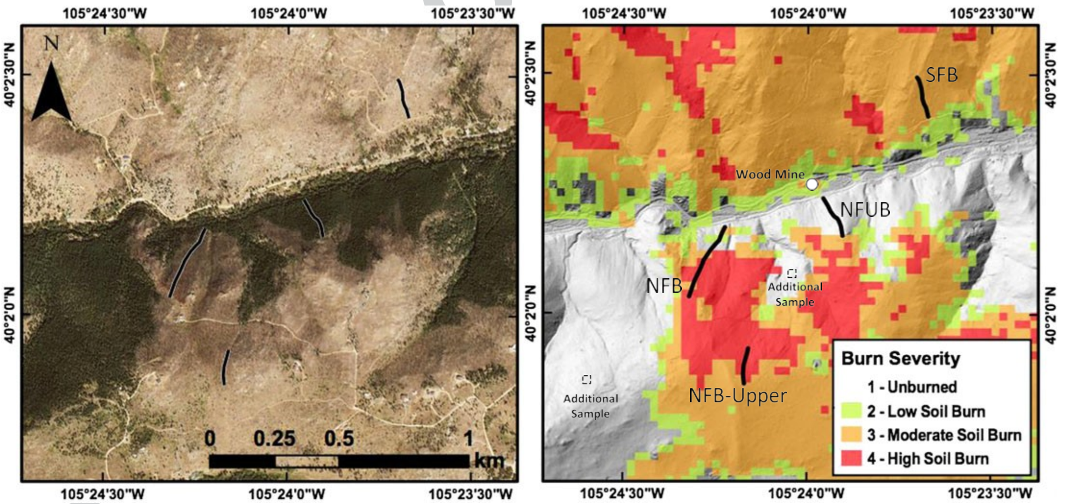

Figure 4. Burn intensity map of the study site with locations of the three soil catena transects. NFB, north-facing burned slope; SFB, south-facing burned slope; NFUB, north-facing unburned slope (control). Boxes indicate where additional reference soil cores were collected outside of the catena transects. Burn severity data based on the normalized burn ratio as part of the USGS FIREMON program (Lutes *et al.*, 2006). [Colour figure can be viewed at wileyonlinelibrary.com]

Table I. Burn severity categories for the study area and hillslope transects mapped in Figure 4

Severity level	dNBR range	Our scale	Transect	Mean	Median	Mode
Regrowth	500 to −101	Not applicable	NFUB	1.44	1	1
Unburned	−100 to +99	1	NFB	3.35	4	4
Low severity	+100 to +269	2	SFB	2.89	3	3
Moderate severity	+270 to +659	3				
High severity	+660 to +1300	4				

Note: dNBR, differenced Normalized Burn Ratio; NFUB, polar (north)-facing unburned slope; NFB, polar (north)-facing burned slope; SFB, equatorial (south)-facing burned slope.

north-facing slopes near Wood Mine generally experienced more intense burning than the equatorial-facing slopes (Figure 4). Furthermore, the north-facing burned areas appeared to be more spatially variable with regard to burn severity than the equatorial-facing burned areas (Figure 4).

After we determined transect positions and lengths, a sampling interval was chosen such that each slope had 8–10 sampling sites. Soils on the hillslopes displayed significant spatial variance in thickness, so two samples were taken at each site along the transect having identical slope positions and thus served as replicates. An ‘A’ sample was taken 5 m directly down-canyon (~east) from the center site, and a ‘B’ sample was taken 5 m directly up-canyon (~west). Additionally, four additional soil reference cores were collected from the unburned north-facing slope in between NFB and NFUB, and another five collected just slightly outside of the Fourmile Burn area approximately 3 km to the southwest of NFB (Figure 4). Bulk soil samples were extracted using a tulip-bulb planter, a reproducible way to sample all of the upper-soil including the litter layer on top with a consistent geometry and a cross-section 7.2 cm in diameter. We sampled from the top of the litter layer down to the depth which the bulb planter could penetrate without solid resistance from boulders or bedrock. Precise sample thickness (typically 12 to 16 cm) was measured for each sample by measuring the depth of the excavated hole, so that each sample volume extracted was known precisely for bulk density determination.

Soil profiles

In addition to bulk soil cores, we sampled several soil profiles to characterize radionuclide behavior with depth in the Fourmile burned and unburned area in 2012 and 2014. One of these profiles, HMF21 was covered by a tarp by USGS researchers in October 2010 after the fire and prior to any rainfall, which allowed the surface ash to be preserved. The tarp was removed just prior to sampling in July 2012. HMF22, directly adjacent to HMF21 (~5 m west), had not been covered, and displayed no ash in the upper 5 cm. The local slope for these pit locations was 33%. Soils were sampled at regular depth increments, generally every 3 to 4 cm, down to ~20 cm. Furthermore, on the NFUB reference slope, we carefully collected the O horizon separately from the upper and lower mineral soil to evaluate the radionuclide partitioning to the combustible organic matter.

Laboratory methods and inventory calculations

We dried the soils at 105°C until they reached a constant mass (24–48 hours), then weighed the sample for total bulk density determination. Samples were then sieved through a < 2 mm stainless steel mesh screen and weighed again to determine the bulk density of the < 2 mm fraction. We ashed a subsample of the < 2 mm fraction in a muffle furnace at 500°C to determine the organic matter content (%) on the north-facing slopes. The < 2 mm soil was homogenized and packed in 40 mL or 60 mL petri dishes which are double-coated with wax to seal radon-222 (^{222}Rn), allowing it to equilibrate with its grandparent radium-226 (^{226}Ra). We measured radionuclides in soil and sediment samples via ultra-low background gamma counting on Canberra Broad Energy 5030 high purity Intrinsic Ge detectors. These detectors are designed with ultra-low background cryostat hardware and remote detector chambers housed in copper-lined 1000 kg+ lead shields. After three weeks, ^{210}Pb, ^{226}Ra, ^{7}Be, and ^{137}Cs were determined at 46 keV, 352 keV (via ^{214}Pb), 477 keV, and 662 keV, respectively. Detector efficiency at these energies for uranium-238 (^{238}U) series radionuclides is determined using certified uranium ore (Canadian Certified Reference Materials Project BL-4a) measured in identical geometry to the samples, but we determined efficiency for ^{137}Cs using a calibrated multinuclide solution containing ^{137}Cs (Isotope Products). To keep counting errors below 8%, samples were typically counted for 48 to 72 hours.

All ^{210}Pb measurements were corrected for self-attenuation using the point-source method (Cutshall *et al*., 1983). At depth in the soil profiles, $^{210}Pb_{ex}$ activities fell to ~88% of that of ^{226}Ra, indicating that approximately 12% of the ^{222}Rn produced in soils escapes to the atmosphere. Excess ^{210}Pb ($^{210}Pb_{ex}$) was thus calculated at each point in soil or sediment profiles using depth distributions of ^{210}Pb and ^{226}Ra, where 88% of the measured ^{226}Ra activity is taken as supported ^{210}Pb (Wallbrink and Murray, 1996). Typical 2-sigma uncertainties for $^{210}Pb_{ex}$ are 2.5 Bq kg^{-1}, which is largely controlled by uncertainty in the supported ^{210}Pb; uncertainties for ^{7}Be and ^{137}Cs are 0.5 and 0.2 Bq kg^{-1}, respectively, and are largely controlled by counting statistics (Kaste *et al*., 2011). We adjusted ^{7}Be values for decay, as its half-life is short enough that non-trivial decay occurred between the collections and processing of samples. We multiplied final concentrations (in Bq kg^{-1}) for all radionuclides by the < 2 mm mass (in kilograms) of the whole soil core extracted, and divided by the area (40.7 cm^{2}) of the coring device to determine soil radionuclide inventories (Bq m^{-2}) of ^{7}Be, ^{137}Cs, and $^{210}Pb_{ex}$ for each landscape point. After processing and analysis, we performed an analysis of variance (ANOVA) and subsequent Tukey Honestly Significant Difference (Tukey HSD) test between the transects for ^{7}Be, ^{137}Cs and $^{210}Pb_{ex}$. We effectively have three populations of soil inventories: NFB, NFUB, or SFB. ANOVA tests were performed on log-normalized data. We measured the specific surface area (in m^{-2} g^{-1}) of select samples using a Brunauer–Emmett–Teller (BET) nitrogen gas adsorption surface area analyzer.

A critical step in applying fallout radionuclides as a tracer of hillslope erosion is to evaluate reference inventories (e.g. Walling and He, 1999), which are effectively the levels of $^{210}Pb_{ex}$ and ^{137}Cs (in Bq m^{-2}) in soils that are supported by atmospheric deposition. To do this, we identified 12 sampling locations on the vegetated NFUB which field notes characterized as having relatively thick (3–7 cm) organic horizons and having moderate to low slope; very steep terrain (slope > 70%) was eliminated as a source of possible reference points. Furthermore, in collaboration with the Boulder Creek Critical Zone Observatory, we established an atmospheric deposition collector at the Gordon Gulch Meteorological Tower at 2530 m elevation and analyzed bulk atmospheric deposition on a approximately six week basis between June 2015 and October 2017. While atmospheric deposition of ^{137}Cs ceased decades ago, ^{210}Pb and ^{7}Be are readily measured in precipitation samples and the direct monthly atmospheric flux measurements can be used to corroborate soil inventories measured at the reference sites for these two radionuclides (Kaste and Baskaran, 2011).

Results

Soil radionuclide concentrations and inventories

All radionuclides were strongly concentrated in the upper 5 to 10 cm of soil; measurements made in soil profiles showed that > 80% of the soil inventory was in the upper 8-cm of soil, and,

> 95% of the inventory was above 12-cm in depth. The soil plot that was covered and protected by a tarp (HMF21) following the 2010 wildfire preserved significantly higher quantities of $^{210}Pb_{ex}$ and ^{137}Cs in the upper ~4 cm of soil compared with a nearby plot that was open (HMF22) and exposed to rainfall on the NFB (Figure 5). The exposed plot had lost 80% of the $^{210}Pb_{ex}$ and 75% of the ^{137}Cs inventory compared with the protected plot by 2012.

To evaluate the depth-distributions of fallout radionuclides in soils at our sites and the partitioning of radionuclides to organic matter and mineral soil, we separately measured the O horizon, upper mineral soil, and lower mineral soil samples for radionuclides at the north-facing forested site. We found that the organic horizon had a very high concentration ratio of $^{210}Pb_{ex}$ to ^{137}Cs of 20.2, while the mineral soil had a comparatively low concentration ratio of two. Organic matter contained ~22 Bq ^{137}Cs kg^{-1}, and given the organic matter pools (Table II) this amounts to ~100 Bq m^{-2} at NFUB, which is a relatively small fraction of the total ^{137}Cs soil inventory that we measured (Table II). Soils on the NFB lost on average approximately 1 kg of organic matter per square meter (*c*. 25%) from the wildfire.

Median inventories for ^{7}Be, ^{137}Cs, and $^{210}Pb_{ex}$ are given in Table II, along with their interquartile ranges (middle 50%) for the NFUB, NFB, and SFB catena transects. Using ANOVA tests, we found a statistically significant difference ($p < 0.05$) between the slopes in the study for all radionuclides. It was found that ^{137}Cs and $^{210}Pb_{ex}$ soil inventories are statistically lowest on the NFB transect, and the variability in these radionuclides on the hillslope as quantified by the interquartile range is relatively larger here as well. Furthermore, $^{210}Pb_{ex}$ and ^{137}Cs exhibited differences between the pairs NFUB-NFB and NFB-SFB, and soil ^{7}Be was significantly higher on NFB. A histogram comparing the inventories measured on NFB and NFUB catena transects shows how the frequency distributions are very distinct (Figure 6).

From the individual hillslope analysis, it was clear that north-facing catenas (mean slope 64%) were indeed steeper than equatorial-facing catena (mean slope 49%), consistent with the general trend of slopes in the region (Graham *et al.*, 2012). Soil ^{137}Cs and $^{210}Pb_{ex}$ were highly variable (Table II, Figure 7) on all slopes measured, and exhibited no clear trend between radionuclide inventory and distance downslope (Figure 7). Linear regressions between slope and ^{210}Pb or ^{137}Cs inventory for all collected samples failed significance tests ($p > 0.05$; $r^2 < 0.01$ where $n = 60$) indicating that slope does not explain local radionuclide losses or gains at these sites. NFUB appears to have a mid-slope maxima in both $^{210}Pb_{ex}$ and ^{137}Cs (Figure 7). NFB has comparatively reduced inventories with higher spatial variability (Figure 6, Table II).

Interestingly the lowermost sampling point on NFB, where two samples were collected from the same slope position in a clearly burned area within meters of each other, had approximately four-fold differences in radionuclide inventories; generally $^{210}Pb_{ex}$ and ^{137}Cs inventories correlate well within each transect.

Table II. Fallout radionuclide inventory (in Bq m^{-2}) and soil organic matter (in kg m^{-2}) median and interquartile ranges (middle 50%) on catena transects

	^{7}Be	^{137}Cs	$^{210}Pb_{ex}$	Organic matter (kg m^{-2})
North-facing unburned (n = 17)				
first quartile	165	1600	3675	2.59
median	225[a]	1835[A]	6890[c]	4.20
third quartile	282	2560	7705	5.29
North-facing burned (upper and lower) (n = 30)				
first quartile	226	179	587	2.55
median	396[b]	415[B]	1340[d]	3.15
third quartile	524	659	2130	3.73
Equatorial-facing burned (n = 17)				
first quartile	310	818	2580	
median	483[b]	1940[A]	5114[c]	
third quartile	670	2710	6290	

Note: Letters ab, AB, and cd indicate where transect means are statistically distinguishable for ^{7}Be, ^{137}Cs, and $^{210}Pb_{ex}$, respectively ($p < 0.05$).

^{137}Cs and $^{210}Pb_{ex}$ reference inventories and erosion rate calculations

Using an average of 12 soil cores from stable, vegetated moderately sloped terrain, we found that the reference inventory for our study area included ^{137}Cs at 1870 ± 670 Bq m^{-2} and $^{210}Pb_{ex}$ at 6410 ± 2200 Bq m^{-2} (median ± σ). The reference

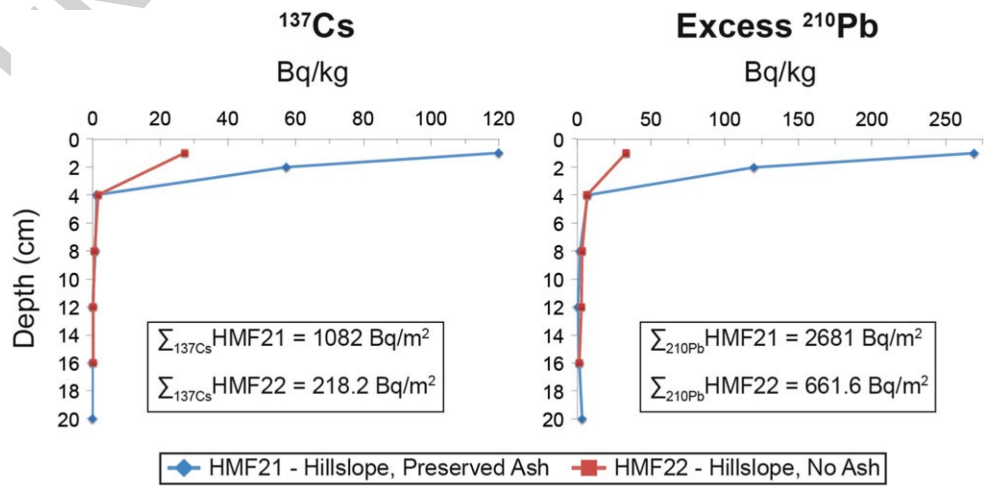

Colour online, B&W in print

Figure 5. Depth-distributions of $^{210}Pb_{ex}$ and ^{137}Cs in soils on two adjacent pits at the same slope position on the north-facing burned slope (NFB). The HMF21 plot was covered by tarp after the 2010 fire, and had a visible layer of ash that was protected from erosion. The HMF22 plot was uncovered and displayed no preserved ash in the upper 5 cm of soil. Total inventories (Σ) show significant radionuclide losses at the uncovered plot. [Colour figure can be viewed at wileyonlinelibrary.com]

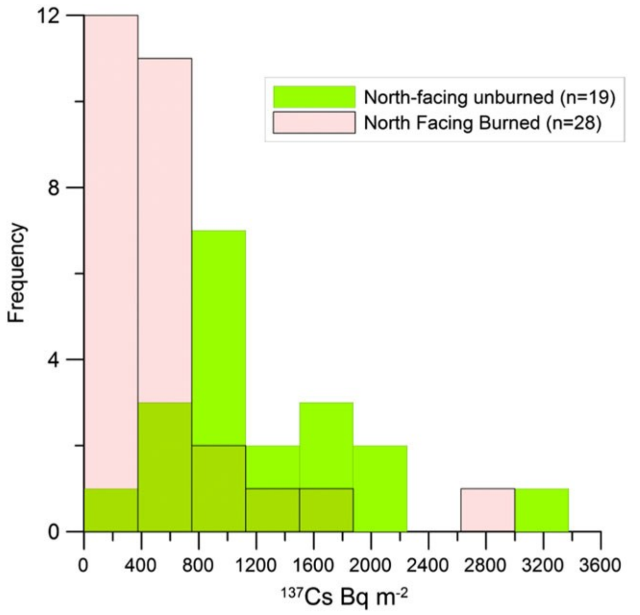

Figure 6. Histogram showing the distribution of ^{137}Cs inventories measured on the north-facing unburned and north-facing burned hillslopes. [Colour figure can be viewed at wileyonlinelibrary.com]

locations had a soil ^{7}Be inventory of 226 ± 180 Bq m^{-2}, but this is lower than SFB and NFB because of the influence of a dense canopy on capturing a significant fraction (up to half) of the atmospheric ^{7}Be (Landis *et al.*, 2014). It is important to note that these inventories are based on the radionuclide concentration (in Bq kg^{-1}) of the < 2 mm soil fraction, multiplied by the bulk density of this size fraction. We analyzed radionuclides in the > 2 mm fraction in three random core samples and found that the ^{137}Cs inventory in the larger fraction was in all three cases relatively small (< 10%), but the same comparison for $^{210}Pb_{ex}$ showed that the coarse fraction contained higher amounts of the total $^{210}Pb_{ex}$ inventory (up to 19%), indicating that coarse organic matter (bark, twigs, leaves) may contain significant ^{210}Pb. Our monthly atmospheric deposition measurements indicated that stable soils would accumulate a steady-state $^{210}Pb_{ex}$ inventory of ~4500 Bq m^{-2} and ^{7}Be inventory of ~375 Bq m^{-2}, which is indistinguishable from the soil inventories measured at our stable reference sites.

Discussion

Fallout radionuclides indicate significant mass loss from the more intensely-burned NFB

We hypothesize that soil erosion magnitude varies by aspect when precipitation events follow wildfire in Fourmile Canyon. Our NFB transect covered soils that were intensely burned based on field evidence (Figure 3) and sampling points here had a median NBR-based burn intensity of a four out a possible four (Table I). In contrast, SFB had a lower burn intensity based on field observations and an NBR median of three, while NFUB was effectively unburned. Soil surfaces on NFB examined in 2013 and 2014 showed substantial evidence of recent

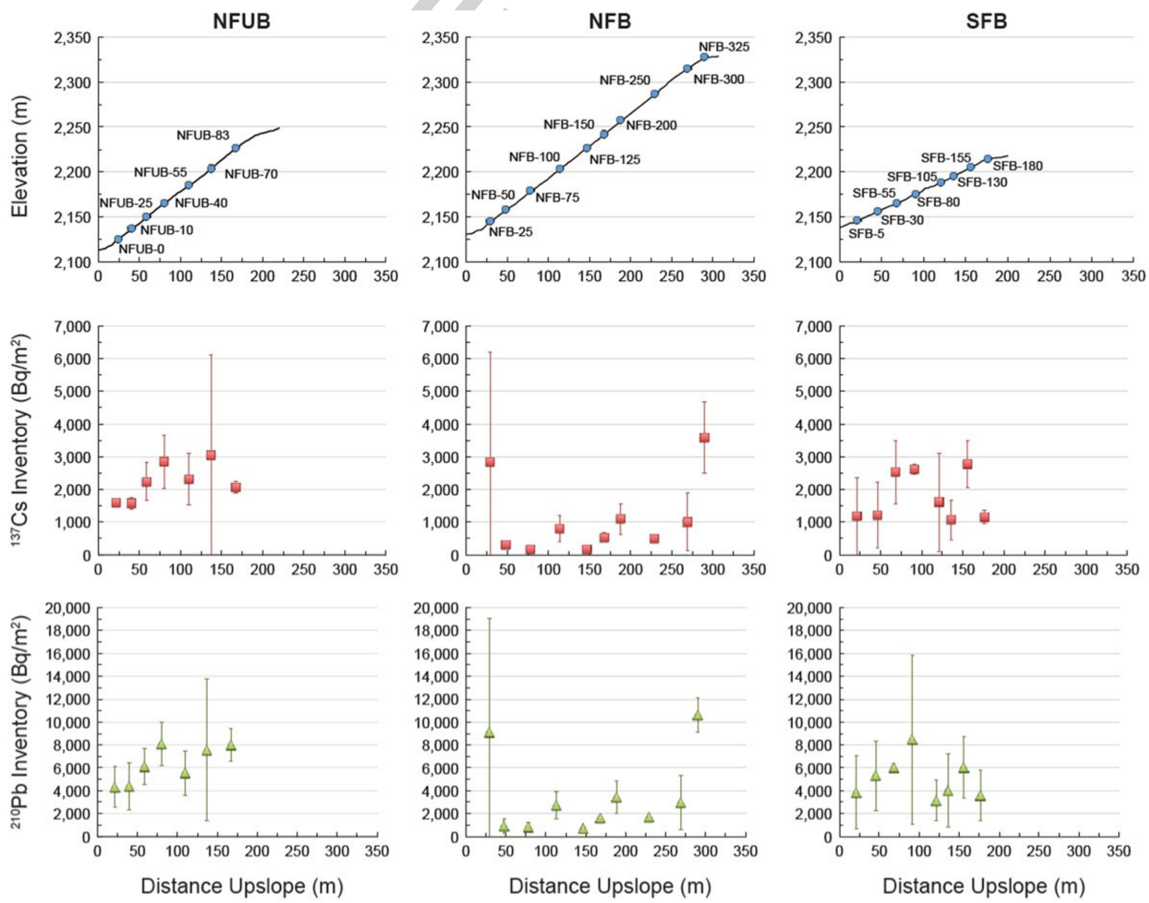

Figure 7. Soil catena transects showing elevation profiles (upper row) and measured radionuclide inventories. Each datapoint represents an average of two soil cores, with error bars showing one standard deviation. [Colour figure can be viewed at wileyonlinelibrary.com]

overland flow that locally caused up to 4 cm of soil loss (Figure 8). Given that the fallout radionuclides are concentrated in the upper fraction of the soil profile (Figure 5), inventories are very sensitive to surface erosion, which is common during years following an intense fire (Moody and Ebel, 2012; Nyman *et al.*, 2013; Ebel *et al.,* 2015). Radionuclide inventories (in Bq m^{-2}) are expected to be relatively lower in areas which eroded, and higher in areas that are accumulating sediment (Walling and He, 1999).

As a tracer, ^{7}Be is useful in showing how the fallout radionuclides are initially introduced to the hillslopes and redistributed with typical precipitation events on short timescales. The short half-life of ^{7}Be limits its tracing power to the last approximate six months, and we find that inventories are higher in SFB and NFB soils compared with the densely vegetated NFUB soils (Table II). Because of radioactive decay, the different hillslope soil ^{7}Be inventories that we observed in 2014 cannot be due to erosion from the rains that followed the fires in 2011–2013, rather, the differences are most likely controlled by forest canopy retention which will be enhanced in NFUB. It is well-documented that vegetation intercepts a significant amount of fallout (Kaste *et al.*, 2011; Landis *et al.*, 2014). Thus, unburned, densely vegetated slopes (i.e. NFUB) are likely to have a considerable amount of ^{7}Be in the forest canopy, where much of it will decay before reaching the ground. The variance in soil ^{7}Be inventories on NFB as measured by the interquartile range relative to the median inventory is 38%, which is consistent with depositional heterogeneity associated with small-scale rainshadowing (Kaste *et al.*, 2011; Kaste *et al.*, 2016).

In sharp contrast to the ^{7}Be inventories, mean ^{137}Cs and $^{210}Pb_{ex}$ soil inventories on NFB were significantly lower than those on the other hillslopes (Table II). As discussed earlier, a possible mechanism for lowering radionuclide inventories on the burned hillslope is the mobilization of ash during and immediately following the wildfire (e.g. Smith *et al.*, 2013). As organic matter burns, radionuclide concentrations at the soil surface can increase by more than an order of magnitude (Owens *et al.*, 2012). While this undoubtedly happened to some extent, we do not believe that this specific process could be responsible for the magnitude of inventory change that we measured. Wildfires effectively burn the organic layer at the soil surface, but intense fast-moving fires typical of this region are unlikely to transfer significant heat down to the mineral soil (Certini, 2005). At the unburned hillslope control, we found that the organic horizon contained relatively low ^{137}Cs, with > 88% of the inventory beneath this combustible layer. In contrast, the $^{210}Pb_{ex}$ was enriched in the O horizon and having the majority of the inventory in this layer. The differential partitioning between these radionuclides and the soil layers is caused by the fact that ^{210}Pb is continuously deposited at the surface but ^{137}Cs was nearly a half-century ago and has had time to diffuse downward.

The fact that the organic layer holds such a small proportion of the ^{137}Cs inventory indicates that the burning and loss of this layer alone could not impact inventories by the magnitude that we observed. On average, we measured ~50% lower ^{137}Cs on NFB, and at some locations up to 90% loss. We believe that the upper mineral soil, which contains 80–85% of the ^{137}Cs must have been eroded to generate these losses, which is consistent with our field observations of rilling in the soils (Figure 8). Moreover, NFB had remarkably consistent soil $^{210}Pb_{ex}$/^{137}Cs and concentrations (Figure 9) which maintained a near-constant value of approximately three across our entire range of inventories. The near-perfect correlation between $^{210}Pb_{ex}$ and ^{137}Cs from the highest to lowest inventories most likely reflects erosion and deposition of sediment containing a relatively constant ^{210}Pb/^{137}Cs activity ratio. This ratio reflects of a mixture of sediment sources but is much more consistent with predominantly mineral soil transport ($^{210}Pb_{ex}/^{137}Cs = 2$ at the reference site) compared with organic matter transport ($^{210}Pb_{ex}/^{137}Cs = 20$ at the reference site). Shortly after the fire, we observed that the ash and the original soil were mixed at the surface, indicating that the distinction between the two was erased relatively quickly. Given that $^{210}Pb_{ex}$ is enriched in the organic litter while ^{137}Cs is enriched in the upper mineral soil, but the total soil inventory response that we measured across all of the NFB positions was identical for the radionuclides (Table II; Figure 9), we argue that the overland flow from the intense storms following the wildfire (Murphy *et al.*, 2015) caused mineral soil (including some ash) erosion.

We interpret the significantly low ^{137}Cs and ^{210}Pb inventories on the NFB to reflect net hillslope-scale soil loss. The NFB < NFUB relationship implicates fire as a clear control on erosion between otherwise similar hillslopes, while the NFB < SFB relationship demonstrates the importance of slope aspect (Table II). These relationships also show that NFUB and SFB are statistically equivalent, implying that the fire made little difference on SFB, most likely because of the relatively lower burn intensity there (Figures 3 and 4). Beyond having lower mean hillslope ^{137}Cs and $^{210}Pb_{ex}$ inventories, the inventory variance within NFB was 57% to 58% for both radionuclides, compared with 38% for ^{7}Be. The higher ^{137}Cs and $^{210}Pb_{ex}$ inventory variance indicates that hillslope distributions of these radionuclides are controlled by processes beyond just atmospheric deposition (Kaste *et al.*, 2016). It seems likely that the rains following the fires in 2011–2013 instigated sediment transport that caused erosion in some areas and deposition in other areas,

Colour online, B&W in print

Figure 8. Exposed roots are other visual evidence of overland flow on the north-facing burned hillslope taken in 2013 (Will Ouimet). [Colour figure can be viewed at wileyonlinelibrary.com]

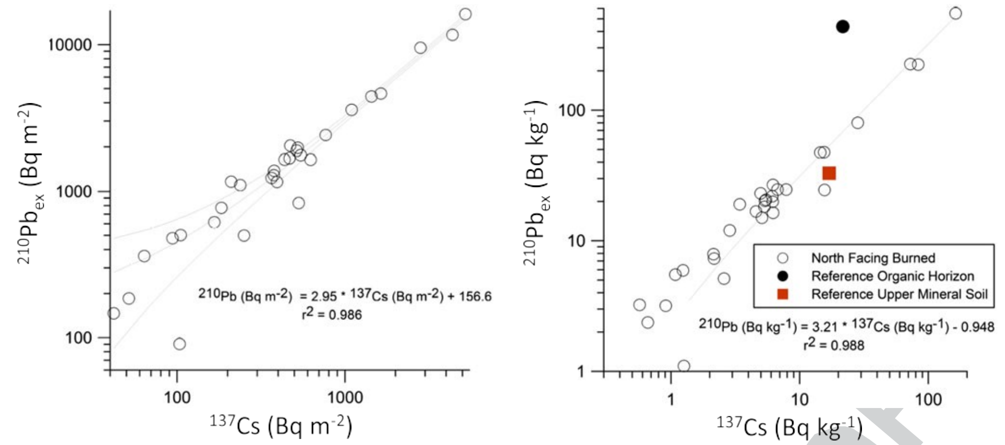

Colour online, B&W in print

Figure 9. Correlations between ^{137}Cs and $^{210}Pb_{ex}$ inventories and concentrations for all north-facing burned sampling points. Also plotted are the concentrations for reference north-facing unburned organic horizon and upper mineral soil samples. Note that both axes are log scaled. [Colour figure can be viewed at wileyonlinelibrary.com]

increasing the variance in ^{137}Cs and $^{210}Pb_{ex}$ while lowering the mean inventory on NFB.

Effects of local slope magnitude on surface erosion and sediment transport

On the more severely burned and eroded NFB, we find no relationship between ^{137}Cs or $^{210}Pb_{ex}$ soil inventories and slope (Figure 10). Thus, burn intensity appears to be the dominant control on soil loss, and sediment transport appears not to be slope limited when intense rains follow fire. Our samples from the upper part of the NFB hillslope transect (NFB-upper on Figure 4) demonstrate this well. We collected eight cores from four sites on a relatively gentle slope (~20%) in the highest burn intensity region, and all samples were significantly depleted in ^{137}Cs (mean ^{137}Cs = 220 Bq m^{-2}). For comparison, 80% of the samples that we collected from steep sections (slope 60–80%)

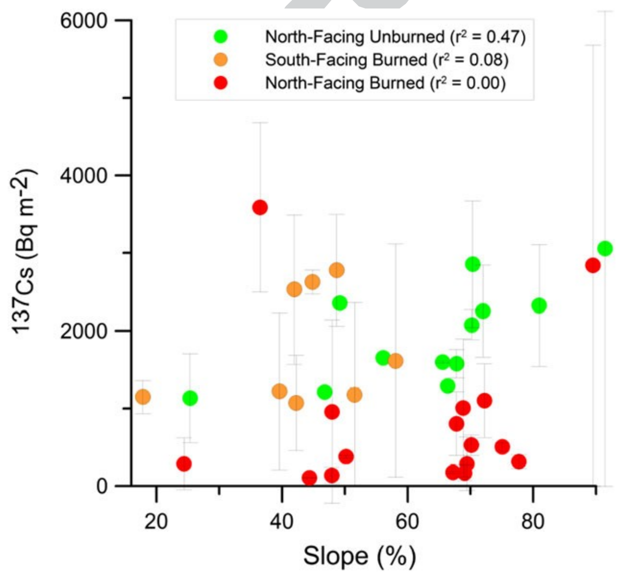

Colour online, B&W in print

Figure 10. Soil ^{137}Cs inventories versus local slope for sampling points on three different hillslope conditions in Fourmile Canyon. Each sampling point is an average of at least two soil cores, and standard deviation on the average is given as a y-error bar. [Colour figure can be viewed at wileyonlinelibrary.com]

of the NFUB had > 1600 Bq ^{137}Cs m^{-2}, indicating geomorphic stability.

It is interesting to note, however, that we find a significant positive correlation ($p < 0.05$) between slope gradient and ^{137}Cs on samples collected from north-facing unburned positions (Figure 10). This is somewhat counterintuitive, because one would expect steeper terrain to shed more soil. However, given that the steepest slopes had ^{137}Cs and $^{210}Pb_{ex}$ inventories higher than we would expect from atmospheric deposition, it seems likely that exposed rocks that are more prevalent on steep terrain trap material eroded from nearby upslope positions. We find no relationship between slope and ^{137}Cs on NFB and a very weak one on SFB (Figure 9). We assume here that the only difference between our sampling points on NFUB and NFB is the burn, and thus conclude that an intense wildfire can 'erase' the control of slope gradient on soil ^{137}Cs (Figure 10).

Geomorphic processes occurring decades prior to the fire also control the radionuclide distributions we measured on all slopes – NFUB has evidence of soil redistribution with areas of erosion and accumulation evident in the ^{210}Pb and ^{137}Cs data (Figures 7 and 10). However, by comparing NFB with NFUB, we can isolate the effects of the 2010 wildfire and subsequent precipitation events on hillslope erosion Because the burn intensity of a wildfire is controlled by fuel abundance (Alexander, 1982), and aspect controls canopy density in Fourmile Canyon, we find that wildfire causes a short-term asymmetry in erosion rates on opposing hillslopes in Fourmile Canyon. North-facing slopes are likely to experience overland flow and sheet erosion after intense fire across the entire range of slopes that we measured (Figure 8).

While sediment transport processes are clearly active on equatorial-facing slopes in Fourmile Canyon, our radionuclide data indicate that this is a more chronic process (e.g. creep from rainsplash or wet–dry cycling) compared with episodic fire-related transport on north-facing slopes. Higher rates of diffusion-like processes on equatorial-facing slopes may result from the lower forest density here. We observed wide variability in ^{137}Cs and $^{210}Pb_{ex}$ inventories on SFB (Table II; Figures 7 and 10); variances for these radionuclides were approximately 50%, compared with 37% for ^{7}Be, and higher than NFUB. While the mean ^{137}Cs and $^{210}Pb_{ex}$ hillslope inventories are indistinguishable from reference values expected from atmospheric fallout, the higher inventory heterogeneity as quantified by the variance is evidence for sediment redistribution as local erosion lowers inventories in some areas and nearby accumulation raises the inventory (Kaste *et al.*, 2016). Using fallout radionuclides, we were unable to detect an episode of erosion from the fire on equatorial-facing slopes, but our data indicate that chronic sediment transport is active on decadal timescales. Others have shown that the equatorial-facing slopes along the Colorado Front Range are more prone to debris flows than north-facing slopes (Ebel *et al.*, 2015).

Timing and magnitude of soil erosion of north-facing burned hillslope soils

While recent works have shown how vegetation and hillslope aspect control debris flow initiation in the Front Range during extreme precipitation (Ebel *et al.*, 2015, Rengers *et al.*, 2016), the role these factors have in controlling overland flow erosion on burned slopes in the region is poorly quantified. Any erosion event since ~1960 would potentially remove ^{137}Cs and $^{210}Pb_{ex}$ from the landscape, but our evidence indicates that most of the radionuclide loss that we measured from NFB happened during the last few years. The soil plot which was protected by a tarp following the fire indicated that a large fraction of ^{210}Pb and ^{137}Cs was in the upper 5-cm of soil in 2010, and the nearby plot without protective cover that was exposed to rainfall had significant (75–80%) inventory reductions by 2012 (Figure 5). This indicates that much of the radionuclide inventory was in the ash that was subsequently swept away during storms in the years immediately following the fire, but this could have been trapped locally downslope.

Significant storage of post-fire mobilized sediment is expected in this region. Moody and Martin (2001) concluded that nearly 70% of the sediment mobilized by storms during the four years following a wildfire in the Colorado Front Range was stored and they estimated a hillslope residence time for this transported material of > 300 years. Our radionuclide inventories indicate points of erosion and deposition (Figures 6 and 9), but net radionuclide losses from NFB indicates significant net soil loss. Weaker correlations between ^{137}Cs and $^{210}Pb_{ex}$ on NFUB ($r^2 = 0.78$) and SFB ($r^2 = 0.36$) indicate that multiple chronic processes, presumably diffusion-like soil transport, have been redistributing sediment rather than the distributions being governed by single recent event. Our short-lived isotope model indicates far higher rates of erosion than were predicted by the *in situ* ^{10}Be model employed by Dethier *et al.* (2014). High sediment loss from NFB leads us to conclude that the magnitude of the erosion event that occurred during the 2011–2014 events was unusual, and, it has been estimated that the seven-day annual exceedance probability for the rainfall in September 2013 was < 0.1% (Murphy *et al.*, 2015).

Given that we observed significantly lower ^{137}Cs and $^{210}Pb_{ex}$ on NFB compared with neighboring hillslope catena transects (Table II), we apply a soil erosion model to estimate sediment loss from NFB. We use ^{137}Cs instead of $^{210}Pb_{ex}$ because based on our measurements of ^{137}Cs in the combustible layer, it would be less impacted by ash transport. However, the near identical inventory response of $^{210}Pb_{ex}$ and ^{137}Cs that we measured on NFB indicates that they had a common mineral carrier (Figure 9). Because of significant variability in fallout radionuclide deposition, it is best to compare populations of soil inventories from 'disturbed' areas with control areas (Zhang, 2014), rather than calculate erosion rates for each specific sampling location. We use the Diffusion and Migration model (Walling and He, 1999, 2001), which compares the mean ^{137}Cs inventory measured in soil cores at NFB with the population of soil cores collected from unburned north-facing sampling locations. This model is calibrated with reference profiles, which are used to determine advection and diffusion rates that describe how ^{137}Cs migrates vertically in the soil with time (Table III). T3

A particle-size factor is used to correct for the fact that fine-grained material is preferentially transported during erosion events Walling *et al.* (2011). We used the preserved top soil from Q8 pit HMF21 (soil + ash mixture) as the mobile phase for the erosion process, and calculate an average net post-1963 sediment loss from NFB to be ~0.4 to 1.2 kg m^{-2}. Given a bulk density of 562 kg m^{-3} this indicates an average of 2 mm across NFB.

Episodic erosion following wildfires in the context of longer-term denudation in Fourmile Canyon

The Front Range of the Rocky Mountains in Colorado, and Fourmile Canyon in particular has been the subject of many geomorphic studies (e.g. Anderson *et al.*, 2015; Murphy *et al.*, 2015). Long-term ^{10}Be-derived erosion rates for similar slopes in nearby Gordon Gulch (Foster *et al.*, 2015) are calculated at ~3 cm every thousand years (0.03 mm yr^{-1}), and ranging from 9 to 31 mm per thousand years (0.009–0.031 mm yr$^{×1}$) in the Front Range as a whole (Dethier *et al.*, 2014). Assuming that all of the radionuclide loss that we observed occurred during the three year period between the wildfire and the 2013 floods, then the erosion rate on NFBs was ~0.7 mm yr^{-1}, which is ~20 times to 80 times the estimated long-term erosion rate.

Erosion rates measured on landscapes recently impacted by fires can be orders of magnitude higher than background, pre-burn conditions (Moody and Martin, 2001). Wildfire can also cause a rapid switch in sediment sources to waterways such as from gullies and river banks to fine topsoil from hillslope surface erosion (Wilkinson *et al.,* 2009). Hillslope aspect has been shown to affect debris flow initiation after wildfire in parts of the Colorado Front Range, particularly because equatorial-facing slopes have lower soil water and drainage capacity (Ebel *et al.,* 2015). Nyman *et al.* (2013) estimated that slope erosion following a 1996 wildfire in the Colorado Front Range was ~200 times background erosion rates, but much of the sediment mobilized from that event was stored. Our use of mean hillslope ^{137}Cs inventory loss gives a net soil erosion magnitude for NFB, it is important to note that based on ^{137}Cs and ^{210}Pb

Table III. Model parameters for using the Diffusion and Migration model to calculate erosion from the north-facing burned slope (NFB)

Model parameter	Value	Units	Origin
^{137}Cs reference inventory	1800 ± 670	Bq m^{-2}	North-facing unburned hillslope cores
Impacted inventory	825 ± 443	Bq m^{-2}	North-facing burned hillslope cores
Downward migration rate	0.14	kg m^{-2} yr^{-1}	Fit of undisturbed profile
Diffusion coefficient	1.15	kg^2 m^{-4} yr^{-1}	Fit of undisturbed profile
Surface area of mobilized sediment	7.7	m^2 g^{-1}	Ash layer analysis
Surface area of original soil	0.98	m^2 g^{-1}	Preserved soil

variance at the on NFB (Table II), local rates of erosion varied by at least a factor of five, and several points on the catena transect indicate local trapping – especially on steeper terrain.

Event frequency is important to consider when calculating longer-term erosion rates from short-term transport episodes. The recurrence interval for fires of the severity of the 2010 event in the Front Range is 30–100 years (Elliot and Parker, 2001; Meyer and Pierce, 2003; Sherriff and Veblen, 2007). While the flooding that occurred in 2013 from the exceptionally intense rainfall is unlikely to coincide with a given past or future fire, strong thunderstorms of similar intensity to those in 2011 and 2012 are common in this part of the Colorado Front Range (Murphy *et al*., 2015). These earlier storms were more temporally proximate to the fire, and had a hydrologic response reflecting low infiltration and high sediment transport (Murphy *et al*., 2015) likely responsible for much of the hillslope soil erosion that we traced with radionuclides. Given that summer storms in the Front Range tend to occur in the months directly following those with the highest wildfire activity (Murphy *et al*., 2015), it is reasonable to assume that a given fire in this region will be followed shortly by moderate to intense storms. Thus, it follows that an erosion event equivalent to the one we measured should occur in the same frequency range as severe wildfire (30–100 years).

Given this 30 to 100 year fire frequency, we would predict a long-term erosion rate of 0.007 to 0.022 mm yr^{-1}, which is remarkably consistent with both the established long-term rate and the rate at which debris flows are thought to exhume sediment in the channels in this area (Anderson *et al*., 2015). Debris flows in crystalline bedrock basins like Fourmile Canyon during the 2013 storms alone removed an average of 1.4 mm of sediment from hillslopes in the region, but also resolved to a long-term rate of ~0.004 mm yr^{-1}, given a recurrence interval of ~300 years for the storm (Anderson *et al*., 2015). As such, it seems likely that rainstorms of moderate intensity or greater following wildfire are a significant driver of long-term erosion rates in this region, and one should expect an increase in the incidence and/or severity of wildfires to notably increase the long-term erosion rate.

While our study indicates that hillslope aspect in the Colorado Front Range controls the post-fire soil erosion response, role of fires on the evolution of the critical zone needs further examination. An average increase of ~0.9°C in the Front Range since the 1970s has resulted in reduced winter precipitation, earlier snowmelt, warm springs, and long, dry summers; ideal conditions for wildfire. This has caused vegetation to become drier, earlier, increasing the fire season by 78 days on average. Accordingly, wildfires have increased four-fold in both frequency and magnitude since 1970, while the area burned has increased by 6.5 times (Westerling *et al*., 2006). Based on the relationship we observed between fire and erosion events in Fourmile Canyon, an increase of this degree has the potential to substantially change future erosion rates.

Conclusions

Given that wildfire frequency is predicted to increase in the coming years, it is critical to quantify the effects that this environmental driver can have on runoff, sediment generation, and soil erosion rates on the critical zone across different landscapes. By sampling soils for fallout radionuclides shortly after the 2010–2013 wildfire and precipitation events in Fourmile Canyon, Colorado, we find that the NFB shows significant evidence of net erosion and soil redistribution, while SFB and NFUB show evidence of sediment redistribution but no measurable net soil loss using the fallout technique. We find that slope magnitude has little effect on the erodibility of soil, but fire intensity, which is controlled by vegetation density and thus aspect, is the dominant control. Locally, we observed up to 4 cm of recent erosion on hillslopes, but much of this was trapped nearby. Average sediment losses from the NFB during 2011–2013 are on the order of 1 kg m^{-2} (2 mm), which is over an order of magnitude larger than annual background erosion rates. Our results support the hypothesis that hillslope aspect and specifically landscape-scale vegetation density can control the geomorphic response of upland soils to wildfires.

Acknowledgements—This research was funded by the Keck Geology Consortium (NSF EAR-1062720) and the NSF Geomorphology and Land Use Dynamics Program (NSF EAR-1401260).

Boulder County Parks and Open Space and USDA Forest Service provided access to public lands. The authors thank Omar Kaufman who assisted with the fieldwork, and Sheila Murphy and Deborah Martin (US Geological Survey, Boulder, CO) who helped with the soil plot experiments.

References

Alexander ME. 1982. Calculating and interpreting forest fire intensities. *Canadian Journal of Botany* 60: 349–357. https://doi.org/10.1139/b82-048.

Anderson SP, Anderson RS, Hinckley ELS, Kelly P, Blum A. 2011. Exploring weathering and regolith transport controls on Critical Zone development with models and natural experiments. *Applied Geochemistry* 26: S3–S5. https://doi.org/10.1016/j.apgeochem.2011.03.014.

Anderson SW, Anderson SP, Anderson RS. 2015. Exhumation by debris flows in the 2013 Colorado Front Range storm. *Geology* 43(5): 391–394. https://doi.org/10.1130/G36507.1.

Brantley SL, DiBiase RA, Russo TA, Shi Y, Lin H, Davis KJ, Kaye M, Hill L, Kaye J, Eissenstat DM, Hoagland B, Dere AL, Neal AL, Brubaker KM, Arthur DK. 2016. Designing a suite of measurements to understand the critical zone. *Earth Surface Dynamics* 4: 211–235. https://doi.org/10.5194/esurf-4-211-2016.

Befus KM, Sheehan AF, Leopold M, Anderson SP, Anderson RS. 2011. Seismic constraints on critical zone architecture, Boulder Creek Watershed, Front Range, Colorado. *Vadose Zone Journal* 10: 915–927. https://doi.org/10.2136/vzj2010.0108.

Burnett BN, Meyer GA, McFadden LD. 2008. Aspect-related microclimatic influences on slope forms and processes, northeastern Arizona. *Journal of Geophysical Research* 113: 1–18. https://doi.org/10.1029/2007JF000789.

Certini G. 2005. Effects of fire on properties of forest soils: a review. *Oecologia* 143: 1–10. https://doi.org/10.1007/s00442-004-1788-8.

Campbell RE, Baker MB Jr, Ffolliott PF, Larson FR, Avery CC. 1977. *Wildfire Effects on a Ponderosa Pine Ecosystem: An Arizona Case Study*, US Department of Agriculture, Forest Service: Rocky Mountain Forest and Range Experiment Station, Research Paper RM-191. USDA: Washington, DC.

Cutshall NH, Larsen IL, Olsen CR. 1983. Direct analysis of Pb in sediment samples: self-absorption corrections. *Nuclear Instruments and Methods* 206: 309–312.

Dethier DP, Ouimet W, Bieman PR, Rood DH, Balco G. 2014. Basins and bedrock: spatial variation in ^{10}Be erosion rates and increasing relief in the southern Rocky Mountains, USA. *Geology* 42: 167–170. https://doi.org/10.1130/G34922.1.

Doerr SH, Shakesby RA, Walsh RPD. 2000. Soil water repellency: its causes, characteristics and hydro-geomorphological significance. *Earth-Science Reviews* 51: 33–65.

Douglas MW, Maddox RA, Howard K, Reyes S. 2004. *The North American Monsoon*. NOAA/National Weather Service, Climate Prediction Center: Reports to the Nation on our changing planet. NOAA: Silver Spring, MD.

Ebel BA, Rengers FK, Tucker GE. 2015. Aspect-dependent soil saturation and insight into debris-flow initiation during extreme rainfall in the Colorado Front Range. *Geology* 43: 659–662. https://doi.org/10.1130/G36741.1.

Eidenshink J, Schwind B, Brewer K, Zhu Z, Quayle B, Howard S. 2007. A project for monitoring trends in burn severity. *Fire Ecology* 3(1): 3–21.

Elliot JG, Parker RS. 2001. Developing a post-fire flood chronology and recurrence probability from alluvial stratigraphy in the Buffalo Creek watershed, Colorado, USA. *Hydrological Processes* 15: 3039–3051.

Foster MA, Anderson RS, Wyshnytzky CE, Ouimet WB, Dethier DP. 2015. Hillslope lowering rates and mobile-regolith residence times from in situ and meteoric 10Be analysis, Boulder Creek Critical Zone Observatory, Colorado. *Geological Society of America Bulletin* 127(5–6): 862–878.

Graham R, Finney M, McHugh C, Cohen J, Calkin D, Stratton R, Bradshaw L, Nikolov, N. 2012. *Fourmile Canyon Fire Findings*, US Department of Agriculture, Forest Service: Rocky Mountain Research Station, General Technical Report RMRS-GTR-289. USDA: Washington, DC.

Hinckley ELS, Ebel BA, Barnes RT, Anderson RS, Williams MW, Anderson SP. 2012. Aspect control of water movement on hillslopes near the rain-snow transition of the Colorado Front Range. *Hydrological Processes* 28: 74–85. https://doi.org/10.1002/hyp.9549.

Kaste JM, Baskaran M. 2011. Meteoric ^{7}Be and ^{10}Be as process tracers in the environment. In *Handbook of Environmental Isotope Geochemistry*, Baskaran M (ed). Springer: Berlin; 61–85 DOI: https://doi.org/10.1007/978-3-642-10637-8_5.

Kaste JM, Heimsath AM, Hohmann M. 2006. Quantifying sediment transport across an undisturbed prairie landscape using cesium-137 and high resolution topography. *Geomorphology* 76: 430–440. https://doi.org/10.1016/j.geomorph.2005.12.007.

Kaste JM, Elmore AJ, Vest KR, Okin GS. 2011. Beryllium-7 in soils and vegetation along an arid precipitation gradient in Owens Valley, California. *Geophysical Research Letters* 38: 1–6. https://doi.org/10.1029/2011GL047242.

Kaste JM, Elmore AJ, Vest KR, Okin GS. 2016. Groundwater controls on episodic soil erosion and dust emissions in a desert ecosystem. *Geology* 44: 771–774. https://doi.org/10.1130/G37875.1.

Kaufmann MR, Veblen TT, Romme WH. 2006. *Historical Fire Regimes in Ponderosa Pine Forests of the Colorado Front Range, and Recommendations for Ecological Restoration and Fuels Management*. Front Range Fuels Treatment Partnership Roundtable, findings of the Ecology Workgroup.

Landis JD, Renshaw CE, Kaste JM. 2014. Quantitative retention of atmospherically deposited elements by native vegetation is traced by the fallout radionuclides ^{7}Be and ^{210}Pb. *Environmental Science and Technology* 48: 12022–12030. https://doi.org/10.1021/es503351u.

Livens FR, Howe MT, Hemingway JD, Goulding KWT, Howard BJ. 1996. Forms and rates of release of 137Cs in two peat soils. *European Journal of Soil Science* 47: 105–112.

Lovering TS, Goddard EN. 1950. *Geology and Ore Deposits of the Front Range Colorado*, USGS Professional Paper 223. Reston, VA: US Geological Survey.

Lutes DC, Keane RE, Caratti JF, Key CH, Benson NC, Sutherland S, Gangi LJ. 2006. *FIREMON: Fire Effects Monitoring and Inventory System*, US Department of Agriculture, Forest Service: Rocky Mountain Research Station, General Technical Report RMRS-GTR-164-CD. USDA: Washington, DC.

Mabit L, Benmansour M, De W. 2008. Comparative advantages and limitations of the fallout radionuclides ^{137}Cs, ^{210}Pb$_{ex}$, and ^{7}Be for assessing soil erosion and sedimentation. *Journal of Environmental Radioactivity* 99: 1799–1807. https://doi.org/10.1016/j.jenvrad.2008.08.009.

Meyer GA, Pierce JL. 2003. Climatic controls on fire-induced sediment pulses in Yellowstone National Park and central Idaho: a long-term perspective. *Forest Ecology and Management* 178: 89–104.

Miller JD, Thode AE. 2007. Quantifying burn severity in a heterogeneous landscape with a relative version of the delta Normalized Burn Ration (dNBR). *Remote Sensing of Environment* 109: 66–80. https://doi.org/10.1016/j.rse.2006.12.006.

Marqués MA, Mora E. 1992. The influence of aspect on runoff and soil loss in a Mediterranean burnt forest (Spain). *Catena* 19: 333–344.

Moody JA, Ebel BA. 2012. Hyper-dry conditions provide new insights into the cause of extreme floods after wildfire. *Catena* 93: 58–63. https://doi.org/10.1016/j.catena.2012.01.006.

Moody JA, Martin DA. 2001. Initial hydrologic and geomorphic response following a wildfire in the Colorado Front Range. *Earth Surface Processes and Landforms* 26: 1049–1070. https://doi.org/10.1002/esp.253.

Moody JA, Martin RG. 2015. Measurements of the initiation of post-wildfire runoff during rainstorms using *in situ* overland flow detectors. *Earth Surface Processes and Landforms* 40: 1043–1056. https://doi.org/10.1002/esp.3704.

Murphy SF. 2006. *State of the Watershed: Water Quality of Boulder Creek, Colorado*, US Geological Survey Circular 1284. Reston, VA: US Geological Survey; 34.

Murphy SF, Writer JF, McCleskey RB, Martin DA. 2015. The role of precipitation type, intensity, and spatial distribution in source water quality after wildfire. *Environmental Research Letters* 10: 1–13. https://doi.org/10.1088/1748-9326/10/8/084007.

Nyman P, Sheridan GJ, Moody J, Smith HG, Noske P, Lane PNJ. 2013. Sediment availability on burned hillslopes. *Journal of Geophysical Research: Earth Surface* 118: 1–17. https://doi.org/10.1002/jgrf.20152.

Owens PN, Blake WH, Giles TR, Williams ND. 2012. Determining the effects of wildfire on sediment sources using ^{137}Cs and unsupported ^{210}Pb: the role of natural landscape disturbance and driving forces. *Journal of Soils and Sediments* 12: 982–994.

Papastefanou C, Manolopoulou M, Stoulos S, Ioannidou A, Gerasopoulos E. 2005. Cesium-137 in grass from Chernobyl fallout. *Journal of Environmental Radioactivity* 83: 253–257.

Parsons AJ, Foster IDL. 2011. What can we learn about soil erosion from the use of ^{137}Cs? *Earth-Science Reviews* 108: 101–113. https://doi.org/10.1016/j.earscirev.2011.06.004.

Peet RK. 1981. Forest vegetation of the Colorado Front Range. *Vegetation* 45: 3–75. https://doi.org/10.1007/BF00240202.

Pelletier JD, Harrington CD, Whitney JW, Cline M, DeLong SB, Keating G, Ebert KT. 2005. Geomorphic control of radionuclide diffusion in desert soils. *Geophysical Research Letters* 32: 1–4. https://doi.org/10.1029/2005GL024347.

Perreault LM, Yager EM, Aalto R. 2017. Effects of gradient, distance, curvature and aspect on steep burned and unburned hillslope soil erosion and deposition. *Earth Surface Processes and Landforms* 42: 1033–1048. https://doi.org/10.1002/esp.4067.

Poulos MJ, Pierce JL, Flores AN, Benner SG. 2012. Hillslope asymmetry maps reveal widespread, multi-scale organization. *Geophysical Research Letters* 39: 1–6. https://doi.org/10.1029/2012GL051283.

Reneau SL, Katzman D, Kuyumjian GA, Lavine A, Malmon DV. 2007. Sediment delivery after a wildfire. *Geology* 35: 151–154. https://doi.org/10.1130/G23288A.1.

Rengers FK, McGuire LA, Coe JA, Kean JW, Baum RL, Staley DM, Godt JW. 2016. The influence of vegetation on debris-flow initiation during extreme rainfall in the Northern Colorado Front Range. *Geology* 44: 823–826. https://doi.org/10.1130/G38096.1.

Ritchie JC, McHenry JR. 1990. Application of radioactive fallout cesium-137 for measuring soil erosion and sediment accumulation rates and patterns: a review. *Journal of Environmental Quality* 19: 215–233.

Shakesby RA, Doerr SH. 2006. Wildfire as a hydrological and geomorphological agent. *Earth-Science Reviews* 74: 269–307.

Sheridan GJ, Nyman P, Langhans C, Cawson J, Noske PJ, Oono A, Van der Sant R, Lane PNJ. 2016. Is aridity a high-order control on the hydro-geomorphic response of burned landscapes? *International Journal of Wildland Fire* 25: 262–267. https://doi.org/10.1071/WF14079.

Sherriff RL, Veblen TT. 2007. A spatially-explicit reconstruction of historical fire occurrence in the ponderosa pine zone of the Colorado Front Range. *Ecosystems* 10: 311–323.

Smith HG, Dragovich D. 2008. Post-fire hillslope erosion response in a sub-alpine environment, south-eastern Australia. *Catena* 73: 274–285. https://doi.org/10.1016/j.catena.2007.11.003.

Smith HG, Blake WH, Owens PN. 2013. Discriminating fine sediment sources and the application of sediment tracers in burned catchments: a review. *Hydrological Processes* 27: 943–958. https://doi.org/10.1002/hyp.9537.

Veblen TT, Kitzberger T, Donnegan J. 2000. Climatic and human influences on fire regimes in ponderosa pine forests in the Colorado Front Range. *Ecological Applications* 10: 1178–1195.

Wallbrink PJ, Murray AS. 1996. Distribution and variability of ^{7}Be in soils under different surface cover conditions and its potential for describing soil redistribution processes. *Water Resources Research* 32: 467–476.

Walling DE, He Q. 1999. Improved models for estimating soil erosion rates from cesium-137 measurements. *Journal of Environmental Quality* 28: 611–622.

Walling D, He Q. 2001. Models for deriving estimates of erosion and deposition rates from fallout radionuclide(caesium-137, excess lead-210, and beryllium-7) measurements and the development of user friendly software for model implementation. In *Impact of Soil Conservation Measures on Erosion Control and Soil Quality*, Technical Report IAEA-TECDOC-1665. International Atomic Energy Agency: Vienna; 11–33.

Westerling AL, Hidalgo HG, Cayan DR, Swetnam TW. 2006. Warming and earlier spring increase western U.S. forest wildfire activity. *Science* 313: 940–943. https://doi.org/10.1126/science.1128834.

Wilkinson SN, Wallbrink PJ, Hancock GJ, Blake WH, Shakesby RA, Doerr SH. 2009. Fallout radionuclide tracers identify a switch in sediment sources and transport-limited sediment yield following wildfire in a eucalypt forest. *Geomorphology* 110: 140–151. https://doi.org/10.1016/j.geomorph.2009.04.001.

Yochum, S. E. 2015. Colorado Front Range flood of 2013: peak flows and flood frequencies. *Proceedings, 3rd Joint Federal Interagency Conference on Sedimentation and Hydrologic Modeling*, Reno, NV; 537–548. DOI: 10.13140/RG.2.1.3439.1520

Zhang XCJ. 2014. New insights on using fallout radionuclides to estimate soil redistribution rates. *Soil Science Society of American Journal* 79: 1–8. https://doi.org/10.2136/sssaj2014.06.0261.